Modular protein-oligonucleotide signal exchange

Deepak K. Agrawal [1,2,*] **and Rebecca Schulman**[1,3,4,*]

[1]Department of Chemical and Biomolecular Engineering, Johns Hopkins University, 3400 N Charles St, Baltimore, MD 21218, USA, [2]Department of Bioengineering, University of Colorado Medicine, Aurora, CO 80045, USA, [3]Department of Chemistry, Johns Hopkins University, 3400 N Charles St, Baltimore, Maryland 21218, USA and [4]Department of Computer Science, Johns Hopkins University, 3400 N Charles St, Baltimore, Maryland 21218, USA

ABSTRACT

While many methods are available to measure the concentrations of proteins in solution, the development of a method to quantitatively report both increases and decreases in different protein concentrations in real-time using changes in the concentrations of other molecules, such as DNA outputs, has remained a challenge. Here, we present a biomolecular reaction process that reports the concentration of an input protein *in situ* as the concentration of an output DNA oligonucleotide strand. This method uses DNA oligonucleotide aptamers that bind either to a specific protein selectively or to a complementary DNA oligonucleotide reversibly using toehold-mediated DNA strand-displacement. It is possible to choose the sequence of output strand almost independent of the sensing protein. Using this strategy, we implemented four different exchange processes to report the concentrations of clinically relevant human α-thrombin and vascular endothelial growth factor using changes in concentrations of DNA oligonucleotide outputs. These exchange processes can operate in tandem such that the same or different output signals can indicate changes in concentration of distinct or identical input proteins. The simplicity of our approach suggests a pathway to build devices that can direct diverse output responses in response to changes in concentrations of specific proteins.

INTRODUCTION

Detecting the presence and relative abundance of different types of proteins is of key importance for diagnostics, biological science, and bioengineering and synthesis. While there are multiple methods for precisely measuring the concentration of proteins in a sample, such as immunosorbent assays (ELISA) (1,2), mass spectrometry (3,4) or western blot (5), these assays cannot be used for 'in situ' protein de-

tection during a chemical process, reaction or within a biological system. In addition, most of these assays require sample processing in which the detected protein cannot be recovered, and thus these assays are not capable of performing real-time readouts. In many cases, it would be helpful to measure the concentration of a protein *in situ* over the course of a reaction, such as to monitor pharmacokinetics (6,7). Ideally, these readouts could also be used to direct the course of the reaction going forward, such as via the release of a specific molecule. In the case of pharmacokinetic monitoring, such a system might conceivably regulate drug release or uptake. Sensors or transducer of this form might also be used for the development of devices to process multiple inputs dynamically to produce diverse output responses.

In vivo, molecular sensors, such as protein receptors, detect protein signals and process and amplify them using molecular cascades (8–10). Molecular circuits consisting of transduction elements might perform similar tasks to allow for *in situ* sensing (11). These insights have led to the development of *in situ* sensing mechanisms that use genetic circuits to process multiple input signals to qualitatively report on protein concentrations inside cells (12–14).

Recent advances in synthetic biology have yielded low-cost short DNA oligonucleotides as a powerful, versatile programmable material to construct sophisticated molecular circuits that relay on hybridization-based strand-displacement reactions (15–18), suggesting that such circuits might be useful to create simple reporting mechanisms that could be used *ex vivo*. Using this strategy, *in situ* protein detection methods have been developed that can translate the presence of a protein into a DNA oligonucleotide strand while using strand-displacement reactions for signal transduction (19,20). In particular, by combining the specificity of DNA aptamers and programmability of DNA strand-displacement reactions, programmable and modular sensing assays have developed that are capable of detecting multiple proteins simultaneously with ultra-low sensitivity (21–24). However, none of these methods resulted in a modular scheme that can be readily available to rapidly translate dynamic changes in the concentration of a protein into a pro-

grammable molecule. The rise and fall of protein concentrations is a key element of cellular signaling using proteins and could also be a key signal for monitoring synthesis or other chemical processes *in situ* using sensors.

Here, we describe a simple sensing mechanism for *in situ* sensing of a protein concentration's rise and fall. This is achieved by using a molecular circuit where the output concentration of a specific DNA sequence rises and falls in a predictable way in response to changes in input protein concentration such that the output is a quantitative indicator of the input protein's concentration. The circuit is composed of an aptamer coupled to a toehold-mediated DNA strand-displacement cascade. Critically there is no restriction on the sequence of the output strand or requirement that it bind to or interact with the protein input, allowing this mechanism to be modularly coupled to a downstream process. We demonstrate that this mechanism can be used to sense different proteins to change the concentrations of DNA strands with different sequences separately and in tandem, and that the circuit can quantitatively react within minutes to both increases and decreases in protein concentrations. Such a characteristic can allow the exchange process to translate input concentrations of many kinds of proteins into oligonucleotide concentrations. These oligonucleotides can then serve as inputs for a growing variety of analytical systems for molecular logic (25), signal modulation (26), or within synthetic gene networks (27) where the concentration of the oligonucleotide initiates or controls the process.

DESIGN

Our goal was to construct a reversible process of biomolecular reaction network where variation in the input protein concentration dynamically changes the concentration of a DNA oligonucleotide. In particular, the sequence of the DNA oligonucleotide should not depend on the identity of the input protein. Further, these reaction networks should be modular such that multiple sensors can translate the concentrations of different input proteins into the concentrations of different oligonucleotides in a single pot reaction. Finally, a predictable input–output response is desired such that for a given output, one can determine how much input was present.

One key requirement for developing such an exchange process for a specific protein is the existence of a DNA aptamer that reversibly and selectively binds to the specific protein with high affinity. Reversible binding between the aptamer and its target is required to detect both rises and falls in protein concentration. Moreover, high affinity binding between the aptamer and the sensing protein is a key determinant of the range of concentrations of protein that can be sensed. The free concentration of the aptamer can then be translated into a DNA oligonucleotide output using a cascade of DNA strand-displacement reactions (28). Such an architecture would allow us to develop a process in which an output signal can then be produced by incorporating a downstream process in response to different proteins (Figure 1A), or different output signals for the same input protein (Figure 1B).

The exchange process we develop is divided into two stages based on their operations. The first stage is a recognition stage that uses reversible aptamer-protein binding (Figure 2). The second stage is a transduction stage, where a change in the concentration of free aptamer is processed into a change in the free concentration of a DNA output strand. The second stage uses a series of toehold-mediated strand-displacement reactions that provide enough freedom such that the sequence of the DNA oligonucleotide output has no sequence in common with the sequence of the original aptamer (Figure 2).

In order for the output to reflect changes in concentration of the input protein accurately, in the recognition stage, the reaction between aptamer and protein should reach equilibrium much faster than any other reactions in the transduction stage. When this is true, the concentration of aptamer not bound to the protein (free aptamer) is a well-defined function of the total aptamer concentration, the protein concentration and the dissociation constant (K_d) of the aptamer–protein reaction. Using this K_d value, we can therefore choose the aptamer concentration such that specific small changes in the concentration of the input protein within particular ranges can produce specific changes in the concentration of aptamer not bound to a protein.

The transduction stage allows the free concentration of aptamer to control the free concentration of a DNA output strand with a sequence (Figure 2). In a coupled system, the concentration of this free output strand should vary precisely with the precise concentration of the input proteins, without any requirement that the output strand shares a sequence in common with the original aptamer. This means that the sequence of the output strand can be selected almost independent of the sensing protein. This coupled system therefore forms a modular exchange process that can be readily adapted to detect different proteins and transduce the detection signal into the concentration of a strand that can control a distinct downstream process.

Designing the exchange process

In our design, to produce a modular output, a DNA aptamer not bound to its target protein should react with a partially single-stranded region of a double-stranded DNA complex in the first step of the transduction stage (Figure 2). The output of this reaction, which is a single-stranded DNA, then reacts with a different double-stranded DNA complex in the second step to produce a single-stranded DNA output with the sequence that can be chosen largely independent of the sequence of the original DNA aptamer.

To achieve this operation, we divided the aptamer sequence into short domains. We added a *d* domain at the 5′-end of the original aptamer and divided the original sequence of the aptamer into *c*, *b* and *tb* domains. Domain *tb* is a short toehold domain that serves as a nucleation site for a toehold-mediated branch migration reaction with the species involved in the transduction portion of the process (28). Domain *d* mediates the interaction of the free aptamer with the complexes that perform the sequence transduction and is part of the sequence of the output strand in the two-step reaction cascade (Figure 2). Note that an interaction between the *d* domain and the original aptamer sequence
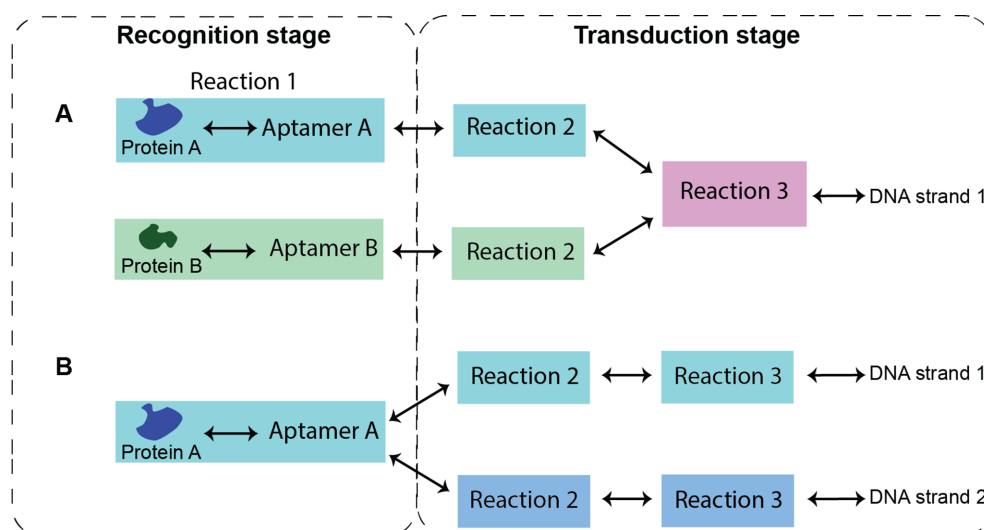
Figure 1. Block diagram representation of protein-oligonucleotide signal exchange processes. Each exchange process consists of a recognition stage where an aptamer targets a specific protein and a transduction stage where reversible toehold-mediated strand-displacement reactions quickly process the free aptamer concentration into the concentration of an output DNA strand. Here, input to Reaction 2 is the free aptamer strand; the presence of the protein reduces the concentrations of free aptamer, which in turn changes the concentration of the output DNA strand. (**A**) Different protein inputs controlling the concentration of the same DNA strand output using two exchange processes with different inputs and the same output. (**B**) Multiple exchange processes controlling the free concentrations of two oligonucleotide outputs that have completely different sequences in response to the same input protein.

can lead to an undesirable folding and/or reduce the affinity of the aptamer toward the protein (29). To avoid this, in this study, domain *d* appended to each aptamer was composed solely of A's and T's, and we used sequences for which secondary structure modeling using NUPACK (30) predicted no interaction between the *d* domain and its respective original aptamer (Supplementary Figure S1).
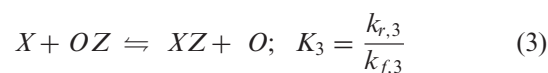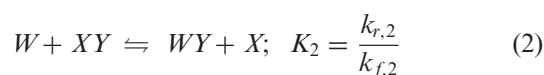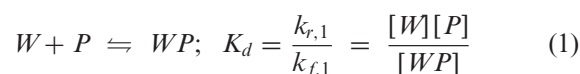
Accurate real-time dynamic sensing requires that all the reactions in the exchange process must be reversible and fast. These characteristics would allow the output of the exchange process to converge quickly to an equilibrium in response to rise and fall in the input concentration. To incorporate these attributes into the exchange process, we used reversible toehold-mediated strand-displacement reactions with at least 4–6 nt long toeholds that correspond to rates of 10^4–10^6 M^{-1}s^{-1} (28).

Moreover, as the transduction stage requires sequence independence between the original aptamer sequence and the sequence of the output strand, a two-step strand-displacement reaction was used (Figure 2). In the first step, the aptamer binds to a complex *X1 Y1* by its toehold domain *tb* and releases strand *X1*. This strand contains only domain *c* that overlaps with the sequence of the original aptamer. Strand *X1* can then react with the *O1Z1* complex, freeing the output strand *O1* and producing *X1Z1* complex. Note that strand *O1* has no overlap sequence with the original aptamer sequence and the only common sequence with the modified aptamer and *O1* strand is the *d* domain. We followed the same design principles to design each exchange process presented in this work.

Kinetic modeling of the exchange process

Our goal in developing modular protein-oligonucleotide signal exchange processes was not to precisely control the concentration of the output in response to variations in the input concentration. Thus, our goal was to produce a process with a well-defined, consistent dose–response curve. For that, we developed a mathematical modeling framework that allowed us to predict the response curve between input and output. This model uses the rate constants of the reactions and the initial concentrations of the molecules involved in the exchange process as the model uses mass-action kinetics of coupled chemical reactions for the reactions:

$$W + P \rightleftharpoons WP; \quad K_d = \frac{k_{r,1}}{k_{f,1}} = \frac{[W][P]}{[WP]} \quad (1)$$

$$W + XY \rightleftharpoons WY + X; \quad K_2 = \frac{k_{r,2}}{k_{f,2}} \quad (2)$$

$$X + OZ \rightleftharpoons XZ + O; \quad K_3 = \frac{k_{r,3}}{k_{f,3}} \quad (3)$$

Each exchange process has *W, P, WP, XY, WY, X, OZ, XZ* and *O* species and a number is associated with each species, which corresponds to the species for that exchange process (ranging from 1 to 4 or for *OZ* 1–2). The symbol [] represents the molar concentration of the species. k_f and k_r represent forward and reverse rate constants respectively, while *K* represents the dissociation constant. Reaction 1 corresponds to the recognition stage of the exchange process where the modified DNA aptamer (*W*) binds to a protein (*P*). Reactions 2 and 3 make up the transduction stage that uses strand-displacement reaction cascade to reflect the changes of free aptamer concentration into the concentration of the output DNA strand (*O*). To be able to model these reactions accurately, the reaction rates ($k_{f,2}$, $k_{r,2}$, $k_{f,3}$, $k_{r,3}$) of Reactions 2 and 3 were estimated using the bimolecular reaction rate constant model (28), which uses the binding energies of each complex from the single-stranded
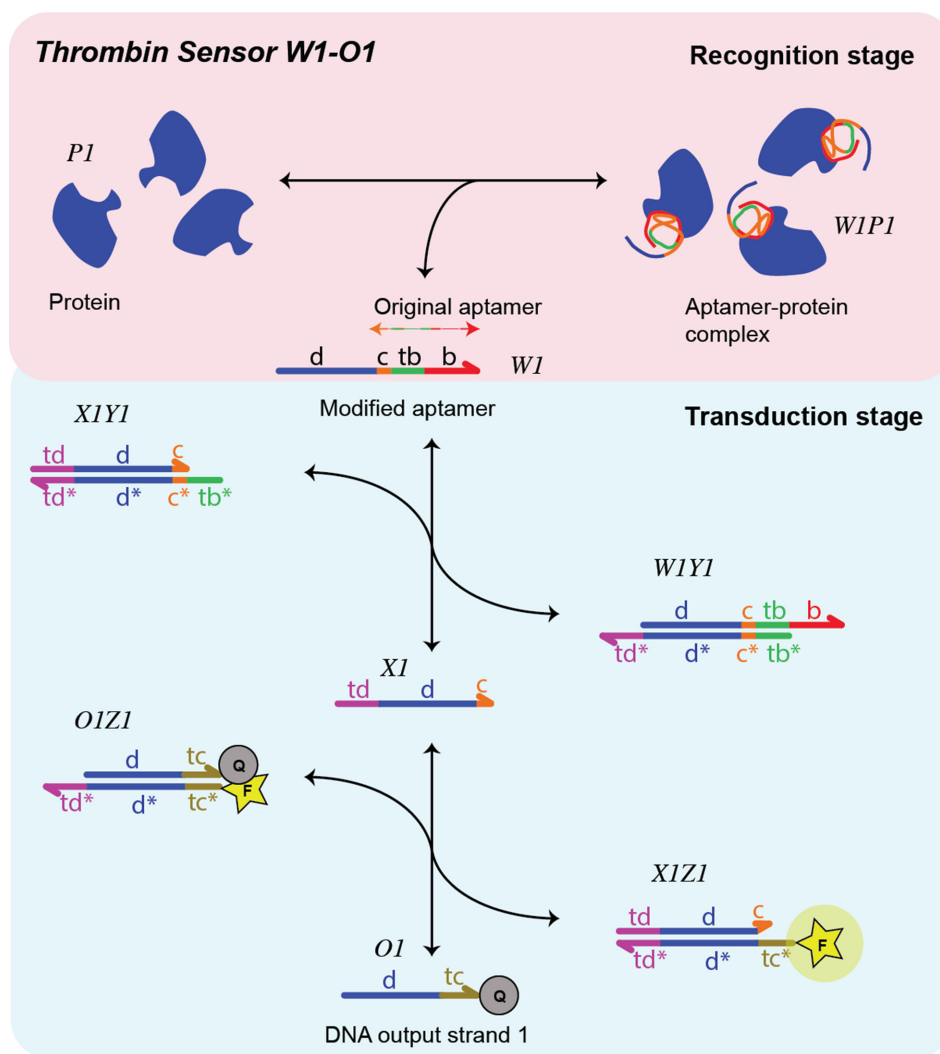
Figure 2. Schematic of a protein-oligonucleotide signal exchange process for dynamically reporting protein concentration as the concentration of an output oligonucleotide with the designed sequence. The concentration of the output strand (*O1*) depends on the concentration of the input protein (*P1*) and the initial concentrations of the sensor components (*W1, X1Y1, O1Z1*). The aptamer (*W1*) binds to the input protein (thrombin for *Sensor W1-O1*) to form an aptamer–protein (*W1P1*) complex. Aptamer strands that are not bound to the protein can react with the *X1Y1* complex, shifting the equilibrium of a reversible reaction so as to change the concentration of free *O1*. [*O1*]$_{\text{free}}$ ranges from [*O1*]$_{\text{total}}$ (when [*P1*] = 0) to 0 (when [*P1*] > ∞). The sequence of the output strand *O1* is independent of the sequence of the original aptamer (Supplementary Data S2) and therefore *O1* sequence can be chosen largely freely in order to couple it to a previously designed downstream process. The forward and reverse reactions within the strand-displacement cascade are each relatively fast because they are mediated by 4–5 base pair (bp) *tb*, or 5 nucleotide *tc* or 6 nucleotide *td* toehold binding domains (28). Typically, for reversible toehold-mediated strand-displacement reactions, these rates vary from 1 M^{-1}s^{-1} (zero nt toehold) to 6 × 10^6 M^{-1}s^{-1} (7 nt toehold or longer) (28). For *Thrombin Sensor W1-O1*, the domains *d, c, b* and *tb* are, respectively, 15, 2, 8 and 5 nt long. Sequences for all the exchange processes are listed in Supplementary Tables S3, S7, S8 and S9. Here and elsewhere [] represents the molar concentration of the species.

species that are involved in a reaction. To calculate these binding energies, we used NUPACK software (30) and then the rate constant model to estimate the rate constants for each exchange process (see Supplementary Data S1; Tables S1 and S2). Because this exchange process uses sequential reactions wherein the output of one reaction serves as the input to another reaction, a simple steady-state analysis might not be an accurate way to predict the output signal with changes in the input aptamer or the protein concentrations. Therefore, an ordinary differential equations (ODEs) based mathematical model was used to predict the kinetics and the steady-state of exchange processes (see Supplementary Data S1).

MATERIALS AND METHODS

Storage

All the DNA strands used in this study were ordered from Integrated DNA Technology, Inc. (U.S.A.) in lyophilized form and were PAGE purified except *Z1, Z2, O1* and *O2* strands that were HPLC purified. Strands *O1, O2* and *Z1, Z2* were labeled with Iowa black FQ quencher and FAM fluorophore dye, respectively, at their 3′ and 5′-ends. For testing the combined operation of *Thrombin Sensor W1-O1* and *Thrombin Sensor W4-O2*, the *Z2* strand was labeled with a HEX fluorophore dye. To determine the equilibrium constant of Reaction 2 for *Thrombin Sensor W1-O1*, the

X1 and *Y1* strands were labeled with FAM fluorophore dye and Iowa black FQ quencher at their 5′ and 3′-ends, respectively. The lyophilized DNA oligonucleotides were diluted in salt-free water and their concentrations were determined by measuring the absorbance at the wavelength of 260 nm on a standard spectrophotometer using the 260 nm extinction coefficient provided by IDT for the respective DNA strands. Human α-thrombin was purchased from Haematologic Technologies, Inc. (Essex, VT) and dissolved in 50% H_2O/glycerol. Recombinant Human vascular endothelial growth factor (VEGF) 165 was purchased from R&D Systems Inc. (U.S.A.) in lyophilized form and was reconstituted at 500 μg/ml in sterile 4 mM HCl containing 0.1% bovine serum albumin. Human α-thrombin and human VEGF 165 are referred to henceforth as thrombin and VEGF respectively. Bovine serum albumin lyophilized powder was purchased from Sigma-Aldrich. All the molecules were stored at −20°C until use.

Electrophoresis mobility shift assay to study TBA15–thrombin and modified TBA15–thrombin interaction

Thrombin Sensor W1-O1 uses modified thrombin-binding aptamer (TBA) to detect thrombin and in response changes the concentration of the output strand *O1* (see Supplementary Data S2). To unfold this aptamer into the lowest energy state ([31]), 20 μM of modified TBA15 (*W1*) was prepared in 1 × reaction buffer (20 mM Tris, 140 mM NaCl, 1 mM Mg^{2+}, 5 mM KCl and 1 mM CaCl with pH 7.4) ([8,21]) of a total volume 50 μl and annealed it by holding the mixture at 90°C for 5 min and then gradually cooling down to 25°C at 1°C/min rate using Eppendorf Mastercycler. This is followed by adding 5 μM of this mixture to separate solutions containing 0, 1, 2.5 and 5 μM thrombin in 1 × reaction buffer components in a total volume of 10 μl. Separate mixtures of original aptamer (TBA15) and thrombin at the same respective concentrations were also made. The samples were incubated for 30 min at 25°C to allow the binding reaction to approach equilibrium, and then were loaded into a 10% polyacrylamide gel (3.25 ml of 40% polyacrylamide solution, 1.3 ml of 10 × reaction buffer, 8.45 ml of MilliQ H_2O, 60 μl of 10% APS and 6 μl of TEMED). Electrophoresis was performed at 4°C for 75 min (100 V) in 1 × running buffer (TBE with 5 mM $MgCl_2$ and 50 mM KCl). The gels were stained with SYBR Gold (ThermoFisher Scientific) for 30 min and subsequently were imaged using a gel imager. To visualize the bands of thrombin, gels were stained with EZBlue (Sigma-Aldrich) for 15 min and the gel was imaged under white light. Analogous protocols were followed to characterize the reaction of other molecules (*b* domain of *W1Y1* or *c* domain of *X1*) with thrombin: pre-annealed *W1Y1* complex (5 μM) or *X1* strands (5 μM) were incubated without and with thrombin (5 μM) for 30 min at 25°C and loaded into a 10% polyacrylamide gel. Subsequently, the resulting gel was stained first using SYBR Gold and then with EZBlue.

Sample preparation for fluorescence spectroscopy experiments

All reactions were performed in 1 × reaction buffer consisting of 20 mM Tris, 140 mM NaCl, 1 mM Mg^{2+}, 5 mM KCl and 1 mM $CaCl_2$ (with pH 7.4) unless otherwise specified. The different components of the exchange process (*W*, *XY*, *OZ* species) were each pre-annealed at 20 μM concentration in 1 × reaction buffer prior to use by heating the mixes to 90°C for 5 min and then cooling down to 25°C at a rate of 1°C/min, and were kept at 25°C until use (within a few hours).

Assay for measuring protein-free response

To measure the aptamer (*W*)–output (*O*) response curve for each exchange process, mixtures containing 100 nM each of pre-annealed *XY* and *OZ* complexes (see the aforementioned note) were prepared in the reaction's buffer. We then added pre-annealed respective aptamer (*W*) to this mixture such that for each aptamer concentration (20, 40, 60 80 and 100 nM), the final solutions were 100 μl in volume and the concentrations of *W*, *XY* and *OZ* were as described in the text. The steady-state fluorescence intensities were measured before and after adding the modified aptamer using the FAM filter of Stratagene Mx3000P real-time thermocycler at 25°C. The changes in the fluorescence intensity that represent the changes in the concentration of the output strand were then converted into concentration using calibration measurements that relate the absolute concentration with the measured fluorescence intensity (see Supplementary Data S3).

Standard protein sensing assay

To test the response of each exchange process to different concentrations of the input protein (0, 20, 40, 60 and 80 nM), the respective input protein (thrombin for *Sensor W1-O1*, *W2-O1*, *W4-O2* and VEGF for *Sensor W3-O1*) was incubated with 100 nM of pre-annealed aptamer at 25°C for 30 min in a total volume of 50 μl containing 1 × reaction buffer for each protein concentration. Subsequently, aptamer–protein mixtures were added into 50 μl solutions each containing 100 nM of pre-annealed *XY* and *OZ* complexes for that sensor in the reaction buffer for a total volume of 100 μl such that the concentrations of sensor components (*W*, *XY*, *OZ*) were as described in the text. We then recorded the changes in the fluorescence intensity before and after adding the aptamer–protein mixture using FAM filter of Stratagene Mx3000P real-time thermocycler at 25°C. The cases wherein the input protein was added in 10 and 50 nM incremental changes; the initial concentrations of each sensor components were 50 nM ([*W*] = [*XY*] = [*OZ*] = 50 nM) and 500 nM ([*W*] = [*XY*] = [*OZ*] = 500 nM), respectively.

Dynamic protein sensing assay

To test the response of *Thrombin Sensor W1-O1* when the thrombin concentration was increased over the course of the reaction in one test tube, a mixture containing 500 nM each of the *X1Y1* and *O1Z1* complexes in the reaction buffer was prepared and the change in the fluorescence intensity was recorded before and after adding 500 nM of *W1* to a total volume of 100 μl. This recording is followed by adding 1 μl of thrombin solution to the mixture such

that it contained 100 nM of thrombin. The fluorescence values were recorded over time until they reached steady-state. To increase the thrombin concentration, the same quantity of thrombin was added several times until the final thrombin concentration of the solution reached 400 nM and after each addition, the fluorescence values were recorded. To test the response of the *Thrombin Sensor W1-O1* to decreases in the thrombin concentration over the course of the reaction in a single test tube, we started with 500 nM of *X1Y1* and *O1Z1* complexes each. These complexes were mixed in reaction buffer and the fluorescence intensity was measured. After this initial measurement, 500 nM of *W1* and 400 nM of thrombin from the stock solutions were added with a total volume of 50 μl. The fluorescence was then recorded until it reached steady-state. To test how the system would respond to decreases in thrombin concentration without altering the concentration of the sensor components (*W1*, *X1Y1*, *O1Z1*), we diluted the reaction mixture by adding 15 μl of a mixture containing 500 nM of each *W1*, *X1Y1* and *O1Z1* to the solution. With each dilution step that corresponds to a decrease in the thrombin concentration, we recorded the steady-state fluorescence value. The process of adding *W1*, *X1Y1* and *O1Z1* and measuring the fluorescence values until a steady-state was achieved was repeated until the final concentration of thrombin reached 182 nM. In both cases, the reported values of the fluorescence were normalized with the fluorescence signal measured when only *X1Y1* and *O1Z1* complexes were present in the mixtures.

Comparing dynamic protein sensing assay with standard protein sensing assay

To validate the results obtained from the dynamic protein sensing assay wherein different thrombin concentrations were added in one test tube, we created reaction mixtures in different test tubes while ensuring that each test tube has the same total volume and concentrations of the molecules as was in the dynamic protein sensing assay for each thrombin concentration. To validated the cases where we increased the thrombin concentration in one test tube (see aforementioned note), we added 0, 100, 200, 300 and 400 nM of thrombin and 500 nM of *W1* (for each case) in different aliquots containing $[X1Y1] = [O1Z1] = 500$ nM in a total volume of 100, 101, 102, 103 and 104 μl, respectively, and recorded the changes in the fluorescence values until they reached a steady-state. To validate the cases where we decreased the thrombin concentration in one test tube, 500 nM of *X1Y1* and *O1Z1* were added in different aliquots containing 182, 211, 250, 308 and 400 nM of thrombin and *W1* of 500 nM (for each case) in a total volume of 120, 95, 80, 65 and 50 μl respectively and the changes in the fluorescence values were recorded.

Characterizing the combined responses of two exchange networks

To test the combined response of *Thrombin Sensor W2-O1* and *VEGF Sensor W3-O1* to different input proteins, 500 nM each of *W2* and *W3* aptamers were incubated, respectively, with different amounts of each thrombin and VEGF

(0, 100, 200, 300 and 400 nM) at 25°C for 30 min to a total volume of 50 μl suspended in the reaction buffer. These mixtures were then added into 50 μl solutions containing 500 nM each of *X2Y2*, *X3Y3* and 1000 nM of *O1Z1* in the reaction buffer for a total volume of 100 μl. The changes in the fluorescence intensity were then recorded at 25°C. We followed the same protocol to measure the combined response of *Thrombin Sensor W1-O1* and *Thrombin Sensor W4-O2* while using the respective sensor components (*W1*, *X1Y1*, *O1Z1* for *Thrombin Sensor W1-O1* and *W4*, *X4Y4*, *O2Z2* for *Thrombin Sensor W4-O2*). Because the *Z1* and *Z2* strands were labeled with FAM and HEX fluorophore dyes, FAM and HEX filters of Stratagene Mx3000P real-time thermocycler were used to measure the changes in fluorescence intensities for *Thrombin Sensor W1-O1* and *Thrombin Sensor W4-O2,* respectively.

RESULTS

Designing and characterizing *Thrombin Sensor W1-O1*

To test whether the exchange process can be used to translate the concentration of an input protein into the concentration of an output DNA strand that has different sequence than the sequence of the original aptamer, we first designed *Thrombin Sensor W1-O1*. This sensor detects human α-thrombin, a serine protease that is involved in activating a coagulation cascade (32). To detect thrombin, the previously studied DNA 15-mer TBA15 (thrombin binding aptamer) (33) was modified to control the concentration of a DNA output strand (*O1*) through the transduction stage. As described in the design methods, we started with dividing the original sequence of the TBA15 aptamer into *c*, *tb* and *b* domains and added a designed 15 nucleotide *d* domain at its 5′-end that was also contained in the output strand (Figure 2). We termed this modified aptamer the *W1* strand. We then designed the *X1Y1* and *O1Z1* complexes such that only *W1* interacts with the thrombin while ensuring that the free *W1* and *X1* can still interact with *X1Y1* and *O1Z1* respectively (see Supplementary Data S2 and Table S3).

We sought to achieve a well-defined dose–response curve for the exchange process by requiring that only Reactions 1–3 govern the operation of the exchange process. That is, we sought that there be no other undesired reactions (also known as crosstalk).

The TBA15 aptamer folds into a tertiary structure, an antiparallel G-quadruplex (33). If any of the species in the cascade share sequence with the original aptamer sequence, and if these species can fold into a similar tertiary structure as the original aptamer, there might be undesired interactions between thrombin and those species. In particular, if the single-stranded *b* domain of the aptamer, which is presented by the *W1Y1* complex, binds to thrombin, the free concentration of the modified aptamer (*W1*) would not be solely determined by the K_d value of the modified aptamer, but also by the undesired reaction between the thrombin and *W1Y1* complex. Similarly, the single-stranded *c* domain of the aptamer, which is presented by the *X1* strand, should also not react with thrombin. We found that these interactions could be avoided by choosing short *b* and *c* domains such that these domains do not fold into any tertiary structures such as a G-quadruplex (Supplementary Data S2).

Binding of the modified aptamer to the input protein in the recognition stage

The first step in characterizing the recognition stage of *Thrombin Sensor W1-O1* was to verify that only the modified aptamer, which contains the TBA15 sequence and *d* domain, binds to thrombin. To test this, a non-denaturing electrophoresis mobility shift assay (EMSA) was used, which measures the ability of thrombin to enter the gel. Thrombin can do so only when it is bound to the aptamer [31]. For that, we added different concentrations of thrombin (0, 1, 2.5 and 5 μM) in the presence of 5 μM of 15-mer TBA15 (see 'Materials and Methods' section; Supplementary Data S2 and Supplementary Figure S2A and B). Similar mixtures were made for the modified TBA15 aptamer (*W1*). In both cases, we observed visible bands in the EZBlue stained gel matrix only when both the aptamer and thrombin were present, suggesting aptamer (either TBA15 or *W1*) thrombin binding (Supplementary Figure S2B and Table S4). Moreover, in cases where we added higher concentrations of thrombin in the presence of a fixed concentration of either aptamer, we observed bands of increased size and intensity in the same gel matrix (Supplementary Figure S2B), indicating increased aptamer–thrombin complex formation. Finally, in the SYBR Gold stained gel matrix, we observed a similar reduction in the band intensities and size with increased thrombin concentration for each aptamer (Supplementary Figure S2A), suggesting a reduction in the free aptamer concentration and hence higher amounts of aptamer–thrombin complex. These results qualitatively suggest that the K_d value of the modified TBA15 aptamer (*W1*) for thrombin should be close to the K_d of the original 15-mer TBA15. To ensure that there are no undesired reactions in the *Thrombin Sensor W1-O1*, we tested whether other species in the exchange process such as the *b* domain of the *W1Y1* complex or the *c* domain of the *X1* strand can interact with thrombin. In the presence of either the *W1Y1* complex or *X1* strand, thrombin was not detected in the gel matrix (Supplementary Figure S3 and Table S5), suggesting that *b* and *c* domains alone have no significant affinity for thrombin.

As a control to show that thrombin enters the gel only when it is bound to either aptamer, we characterized the interaction of thrombin with aptamer in presence of non-aptamer DNA in the same gel matrix (Supplementary Figure S4 and Table S6) while using the same stoichiometry as was used in Supplementary Figures S2 and S3. In free thrombin case, we did not observe any bands suggesting that thrombin alone does not enter the gel. Further, we did not observe any visible change in the band intensities of *X1* strand in the absence and presence of thrombin, suggesting the non-aptamer DNA (*X1* strand) cannot bind to thrombin (Supplementary Figure S4).

Characterizing the transduction stage response in a protein-free environment

The next goal was to characterize the response of the transduction stage, where the free aptamer interacts with a downstream complex to control the concentration of free output strand. To test what concentrations of free aptamer produce what concentrations of the output strand, the concentration

of *W1* was varied while keeping the initial concentrations of *X1Y1* and *O1Z1* complexes at 100 nM each. To be able to readout the concentration of the output strand (*O1*) over the course of the reaction, a fluorophore was added to the 5′-end of the *Z1* strand (FAM unless otherwise mentioned) and a quencher to the 3′-end of the *O1* strand, which is hybridized to *Z1* when it is not free (see 'Materials and Methods' section). Therefore, the fluorescence of the mixture reflects the concentration of free *O1* at the steady-state (Figure 3A; see Supplementary Data S3 and Figure S5).

To predict the concentration of *O1* in response to different concentrations of *W1*, the rate constants of Reactions 2 and 3 for *Thrombin Sensor W1-O1* were calculated and then these rates were fed into an ODE model (see Supplementary Data S1). The simulated response predicted a higher amount of *O1* than the measured values (Supplementary Figure S8). This discrepancy might be caused by the G-quadruplex structure within *W1*, which can prevent *X1Y1* complex from interacting with *W1* via the *tb* domain. Such a hindrance would be expected to reduce the forward rate constant ($k_{f,2}$) of Reaction 2. Such a change cannot be predicted by NUPACK, as NUPACK does not consider the energetics of tertiary structures such as the G-quadruplex.

To validate this hypothesis, we tested the operation of Reaction 2 alone. For that, the *X1Y1* complex was modified such that it has a fluorophore attached to the 5′-end of *X1* strand and a quencher molecule attached to the 3′-end of *Y1* strand (see 'Materials and Methods' section; Supplementary Data S4 and Figure S9A). We then measured the changes in the concentration of the *X1* strand at different concentrations of *W1* in the presence of 250 nM of *X1Y1*. Using the ODE model, we found that the measured response of Reaction 2 closely followed the model data for a $k_{f,2}$ value of 5×10^4 $M^{-1}s^{-1}$ (Supplementary Figure S9B). Notably, this value is much smaller than the value calculated using the kinetic model (2.83×10^6 $M^{-1}s^{-1}$). As an additional verification that this smaller rate was the correct one, a least-squares fitting method was used to determine the $k_{f,2}$ value, which provided the best fit between the model data and the measured protein free response (Reactions 2 and 3) while using the rest of the rates calculated using the rate constant model (28). A close agreement between the model and the data was found when $k_{f,2}$ was 6.49×10^4 $M^{-1}s^{-1}$ (Figure 3A).

Detecting different protein input concentrations

Having validated the operation of recognition and transduction stages of *Thrombin Sensor W1-O1* separately, the next goal was to characterize the behavior of the full exchange process. In this process, an incremental change in the concentration of thrombin should incrementally reduce the amount of *O1*. These changes should be predicted by a model that incorporates the rates of the reaction involved in the transduction stage and the rates of TBA15–thrombin interaction. The rates of the TBA15–thrombin interaction in our models were taken from the literature (34,35) (see Supplementary Table S2). To test that the kinetics of the cascade were consistent with the aggregate kinetics predicted by this model, we varied the thrombin concentration from 0 to 80 nM in the presence of 100 nM of each *W1*, *X1Y1*
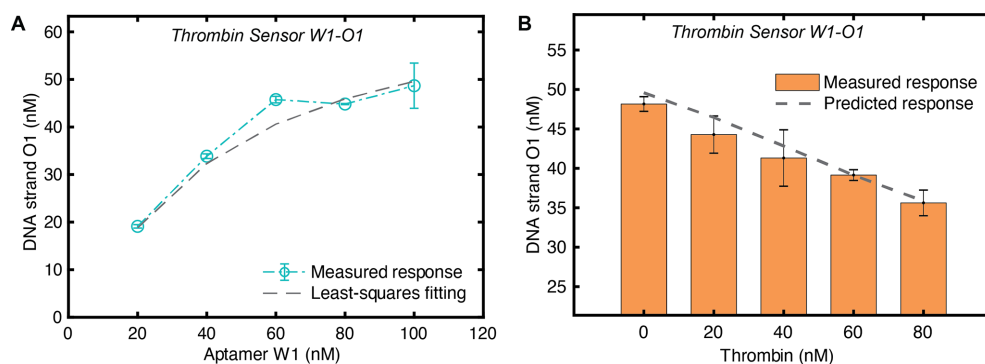
Figure 3. Input protein concentration controls output oligonucleotide concentration through the free aptamer concentration. (**A**) The equilibrium concentration of *O1* in a protein-free environment for *Thrombin Sensor W1-O1* at different concentrations of *W1* while initial concentrations of *X1Y1* and *O1Z1* were 100 nM each. (**B**) The equilibrium concentration of *O1* to different concentrations of thrombin where initial concentrations of *W1*, *X1Y1* and *O1Z1* were 100 nM each. For both experiments, calibrations were used to convert the measured fluorescence intensities into *O1* concentrations (see Supplementary Data S3 and Figure S5). The error bars here and elsewhere were determined using the standard error of the mean of three or more measured responses. Here and elsewhere, an ODE model was used to determine the response of the exchange process without and with protein (Supplementary Data S1). The reaction rates were determined using the biomolecular rate constant model of toehold-mediated strand-displacement (28) except the forward rate constant of Reaction 2 that was determined using the least-squares fitting of the measured protein free response. The aptamer-protein (*W1-P1*) interaction was modeled using the K_d value and forward reaction rate constant ($k_{f,1}$) reported in (34,35) (see Supplementary Data S1).

and *O1Z1* and measured the steady-state fluorescence intensities for each thrombin concentration mixture (see the standard sensing assay in 'Materials and Methods' section). The measured response was almost identical to the response predicted by the model (Figure 3B). Multiple tests of the exchange process produced very similar dose–response curves.

The exchange process should also be able to reliably produce predictable changes in *O1*'s concentration when the thrombin is added in smaller or in larger quantities compared to the values than those reported in Figure 3B. To verify this, we tested the response of *Thrombin Sensor W1-O1* to different ranges of input thrombin concentrations. During these tests, to track the changes in the concentration of the *O1* strand accurately, different initial concentrations of the sensor components (*W1*, *X1Y1* and *O1Z1*) were used (see 'Materials and Methods' section). For each variation in the thrombin concentration, a well-predicted dose–response curve was observed (Supplementary Figure S10).

One of the main design considerations of the reaction cascade is that the free aptamer concentration should entirely control the output strand's steady-state concentration. This requires that thrombin should not interact with any other reactant of the transduction stage. To test this, the operation of the sensor was recorded in the absence of aptamer (*W1*). We observed only a negligible change in the output as a function of thrombin concentrations (Supplementary Figure S11A). Moreover, because the thrombin stock used was dissolved in a 50% H$_2$O/glycerol mix, we also tested whether such a mixture alone would shift fluorescence values. We observed no significant changes in *O1* response to the addition of different amounts of 50% H$_2$O/glycerol mixture (Supplementary Figure S11B).

Detecting dynamic changes in thrombin concentration over the course of a reaction

The reversible nature of the exchange process should allow the concentration of the output strand to change in response to changes in the protein concentration by chang-

ing the output strand's steady-state concentration. To test whether such updates occur, we first characterized how the *Thrombin Sensor W1-O1* responded to increases in thrombin concentration in the same test tube over the course of the reaction. For this, a mixture consisting of 500 nM *W1*, *X1Y1* and *O1Z1* each was prepared, and then thrombin was added to a final concentration of 100 nM to the mixture. The change in the fluorescence was then measured (see dynamics sensing assay in 'Materials and Methods' section). More thrombin was then added in such a manner that the final concentration of thrombin in the mixture reached 200 nM. The output fluorescence decreased after thrombin was added, and decreased each time after more thrombin was added in steps up to a final concentration of 400 nM (Figure 4A).

To determine whether the exchange process can also respond to decreases in the thrombin concentration, a mixture consisting of 500 nM *W1*, *X1Y1* and *O1Z1* species each was prepared to which 400 nM of thrombin was added. To decrease the concentration of the thrombin without changing the effective concentration of the sensor components (*W1*, *X1Y1* and *O1Z1*), a mixture containing 500 nM of the sensor components was added such that the final concentration of thrombin in the mixture was 308 nM while the sensor components remained at 500 nM (see dynamics sensing assay in 'Materials and Methods' section). The fluorescence value was increased after dilution. This was followed by further dilution steps that decreased the thrombin concentration to 250, 211 and then 108 nM, which resulted in a significant increase in the fluorescence value (Figure 4B).

In the standard protein sensing assay, where different concentrations of thrombin were tested in different aliquots, the same reaction volume was used in each aliquot. This allowed us to use a single calibration curve to convert the measured fluorescent signal into the concentration of *O1* (Figure 3, Supplementary Data S3). For the dynamic sensing case (Figure 4), a single calibration curve could not be used to find the changes in concentration of signal from the change in fluorescence because of the final volume of
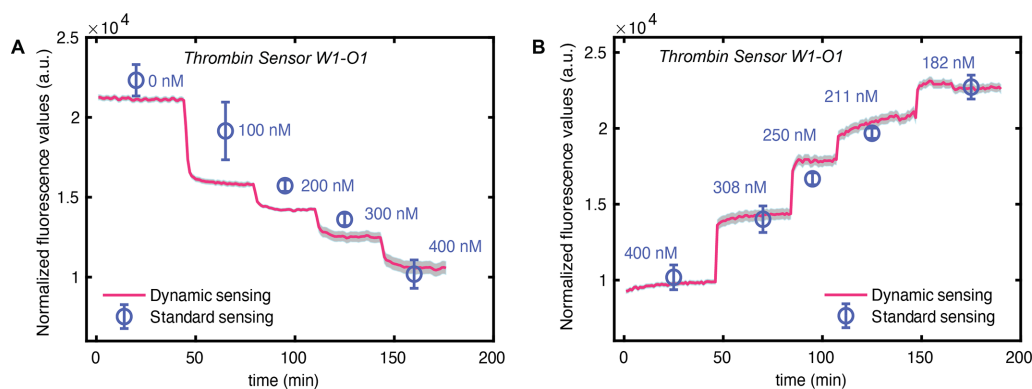
Figure 4. Exchange process can dynamically modulate the output concentration in response to dynamic changes in the protein input concentration over the course of a reaction. Measured fluorescence values of *Thrombin Sensor W1-O1* as a function of thrombin concentration that was either increased or decreased over the course of a single pot reaction through the addition of thrombin or dilution of sensor components, respectively (see dynamic sensing assay in 'Materials and Methods' section). These responses are compared with measurements where for each thrombin concentration a separate mixture was made (standard sensing assay in 'Materials and Methods' section) while maintaining the same volume and molarity of thrombin and sensor components as in the dynamic sensing case (see 'Materials and Methods' section). (**A**) To test how the reversible exchange process responds to increases in thrombin concentration, *X1Y1* and *O1Z1* at 500 nM each were mixed and then 500 nM of *W1* was added. This is followed by the addition of small volumes of thrombin from a concentrated stock in steps to increase thrombin concentration such that the sensor components' concentration was not significantly altered because of the dilution (see 'Materials and Methods' section). (**B**) To test how the exchange process responds to decreases in thrombin concentration, 500 nM of *X1Y1* and *O1Z1* were mixed and then added 500 nM of *W1* followed by 400 nM of thrombin (first step). To reduce the thrombin concentration without altering the concentration of sensor components, this mixture was diluted by adding a fixed volume from a stock of sensor components containing $[W1] = [X1Y1] = [O1Z1] = 500$ nM several times.

the reaction mixture was different (due to the dilution step) for each thrombin concentration. In the instrument that we used in this work to record the fluorescence signal (Stratagene Mx3000P thermocycler), the volume changes the conversion between these two quantities. Therefore, to determine whether the changes in fluorescence after dilution indicated that the exchange process reached the expected equilibrium, for each of the measured values performed above, we prepared mixtures of the sensor components (at 500 nM each) and thrombin such that the final concentration of all the species involved in the exchange process was the same as in the above experiments. For each thrombin concentration, a separate mixture was made by following the standard protein sensing assay (see 'Materials and Methods' section). The fluorescence measurements of these mixtures were consistent with those achieved through either the addition of more thrombin or more sensor components, indicating that the dynamic response of the system shifted the concentration of the output strand to its new equilibrium concentration, as designed (Figure 4).

Producing identical DNA outputs using different aptamers or a different input protein

The modular design of the exchange process suggests that it should be straightforward to design new exchange processes that can produce an output strand of the same sequence as *O1* in response either to a different input protein or that uses a totally different aptamer in the recognition stage compared to *Thrombin Sensor W1-O1*. To demonstrate this capacity of the exchange process, we designed *Thrombin Sensor W2-O1* that detects thrombin concentrations but does so using the DNA 29-mer DNA TBA29 to target thrombin, and *VEGF Sensor W3-O1* that detects the concentration of vascular endothelial growth factor (VEGF) protein.

Unlike TBA15 that binds to thrombin at its fibrinogen exosite and inhibits thrombin catalytic action to promote clotting, DNA aptamer TBA29 binds at the heparin exosite of thrombin with a K_d value of 0.5 nM (36) without alerting thrombin's catalytic activity (37). The *VEGF Sensor W3-O1* used a 25-mer 3R02 DNA aptamer that binds to VEGF at its receptor-binding domain with a K_d value of 0.3 nM (38,39). Similar design guidelines were used to design these new exchange processes as mentioned earlier (see 'Design' Section and Supplementary Data S2 and S5). To produce the same DNA output strand (*O1*) from *Thrombin Sensor W2-O1* and *VEGF Sensor W3-O1* as in *Thrombin Sensor W1-O1*, the sequence of the *d* domain that was added in modified TBA29 and 3R02 aptamers was the same as the sequence added to create the modified TBA15 for *Thrombin Sensor W1-O1* (see Supplementary Tables S3, S7 and S8).

Similar to *Thrombin Sensor W1-O1*, we first characterized the protein-free response of the *Thrombin Sensor W2-O1* and *VEGF Sensor W3-O1* at different concentrations of *W2* and *W3* respectively (Supplementary Figure S12A and B).

To model these exchange processes, we calculated the reaction rate constants for each exchange process and then used these values in the ODE model to determine the sensor response (see Supplementary Data S1 and Supplementary Table S2). The predicted response did not match the measured response in either case (Supplementary Figure S12A and B). Since the aptamers used by these new processes have tertiary structures, the forward rate constants ($k_{f,2}$) that control the interaction rates between the respective aptamer and *XY* complex might be reduced as was observed for *Thrombin Sensor W1-O1*. Therefore, we used the least-squares fitting method to find the best fit for a $k_{f,2}$ value at which the model data follow the protein-free mea-

sured response of each sensor (Supplementary Figure S12C and D).

We then measured the responses of *Thrombin Sensor W2-O1* and *VEGF Sensor W3-O1* separately to different concentrations of their respective input proteins (Thrombin or VEGF) and in the presence of respective sensor components (*W2*, *X2Y2*, *O1Z1* or *W3*, *X3Y3*, *O1Z1*) (Figure 5A and B, respectively). For each exchange process, the measured *O1* concentrations were then compared with the predicted response using the same rates that were used to model the protein-free responses (Supplementary Figure S12C and D; Supplementary Data S1). A close agreement between the measured and predicted response for each exchange process can be seen in Figure 5A and B. By changing the concentrations of the sensor components, we were also able to change the dynamic range of *O1* in response to a set of smaller and larger protein concentrations (Supplementary Figures S13 and S14) compared to Figure 5A and B.

Constructing exchange processes with a distinct output signal

So far, all the exchange processes produced the same output strand *O1* in response to different protein concentrations, irrespective of aptamers used to detect different proteins. As a next step, we sought to build an alternative exchange process that controlled the concentration of an output strand with a different sequence (*O2*) than *O1* strand but did so in response to the same input protein (thrombin) using the aptamer binding partner (TBA15) in *Thrombin Sensor W1-O1*. This was achieved by adding a different *d* domain sequence to the TBA15 aptamer (Supplementary Tables S3 and S9). While designing the component of *Thrombin Sensor W4-O2,* similar design guidelines were followed as those used to design the *Thrombin Sensor W1-O1* (see 'Design' section, Supplementary Data S2 and S6).

A similar approach was followed to characterize and predict the response of *Thrombin Sensor W4-O2* as mentioned for the other exchanges processes. The protein-free response of *Thrombin Sensor W4-O2* is shown in Figure 5C, which was used to compute $k_{f,2}$ while the other rates of the transduction stage were calculated in a similar manner to those for the other cascades (Supplementary Data S1). The measured response of *Thrombin Sensor W4-O2* closely agreed with the predicted response over different ranges of thrombin concentrations (Figure 5D; Supplementary Figure S15). Together, these experiments demonstrate a route to designing a method for translating an input protein concentration into an oligonucleotide output concentration where the input protein and the sequence of oligonucleotide output can be chosen independently.

Simultaneous detection of different proteins and control of the concentrations of different DNA oligonucleotide outputs

One of the advantages of using DNA aptamers and strand-displacement reactions in the exchange process is that DNA aptamers can bind both to the specific proteins and the complementary DNA strands with high specificity. The sequence-specific interactions in the transduction stage make the exchange process operation modular. Because of these attributes, one would expect that these exchange pro-

cess should operate in a similar manner when operated individually or concurrently. To determine whether this is the case, we sought to characterize multiple exchange processes in a single pot reaction to see whether (i) each process could translate the concentration of different input proteins into a common output signal (Figure 1A) or (ii) the same input protein could control the concentrations into different output signals (Figure 1B).

To test the sensor architecture shown in Figure 1A, where two different protein inputs control the same oligonucleotide output, we tested the responses of *Thrombin Sensor W2-O1* and *VEGF Sensor W3-O1*. These sensors detect thrombin and VEGF receptively, and produce the same oligonucleotide output *O1*. For simplicity, both the input proteins were varied by equal amounts while measuring their combined response (see 'Materials and Methods' section). As both of these processes use the *O1Z1* complex in the transduction stage, it was not possible to track the concentration of the output strands of each process separately. As a solution, we relied on our mathematical model to estimate the amounts of *O1* produced by each exchange process (see Supplementary Data S7). The predicted individual and combined responses and the measured combined response of *Sensor W2-O1* and *W3-O1* are shown in Figure 6A. The predicted response of the combined exchange processes followed the measured response closely, suggesting that the two exchange processes work almost independently, and that the model can correctly interpret the concentration of the two input proteins simultaneously and predict the output (Figure 6A).

We finally sought to examine the operation of two exchange processes together that can accurately reflect changes in the concentration of the same input proteins in the concentrations of two different DNA output strands with different sequences (Figure 1B). For this, we tested the operation of *Thrombin Sensor W1-O1* and *Thrombin Sensor W4-O2* that target the same input protein (thrombin) using the same original aptamer (TBA15) but modulate the concentrations, respectively, of *O1* and *O2* strands in response. Because these processes use different *OZ* complexes in the transduction stage, the output of each process was tracked separately using different fluorophore molecules attached to the respective *Z* strand (see 'Materials and Methods' section).

In this new arrangement, *Thrombin Sensor W4-O2* used the HEX fluorophore dye rather than the previous design where FAM fluorophore dye was used. This required characterizing *Thrombin Sensor W4-O2* with HEX fluorophore dye again for different input protein concentrations similarly as was done for *Thrombin Sensor W4-O2* with FAM fluorophore dye (see Supplementary Data S3 and Figure S7). A separate calibration measurement was used to convert the measured fluorescence values into concentrations (see Supplementary Data S3). Subsequently, *Thrombin Sensor W1-O1* and *Thrombin Sensor W4-O2* were tested together in a single pot reaction in the presence of thrombin that was twice the amount of the cases wherein the response of the individual process was recorded (Figure 6B). The combined measured response remained close to the values observed for the individual responses of each sensor. These results demonstrate that the recognition stage of each
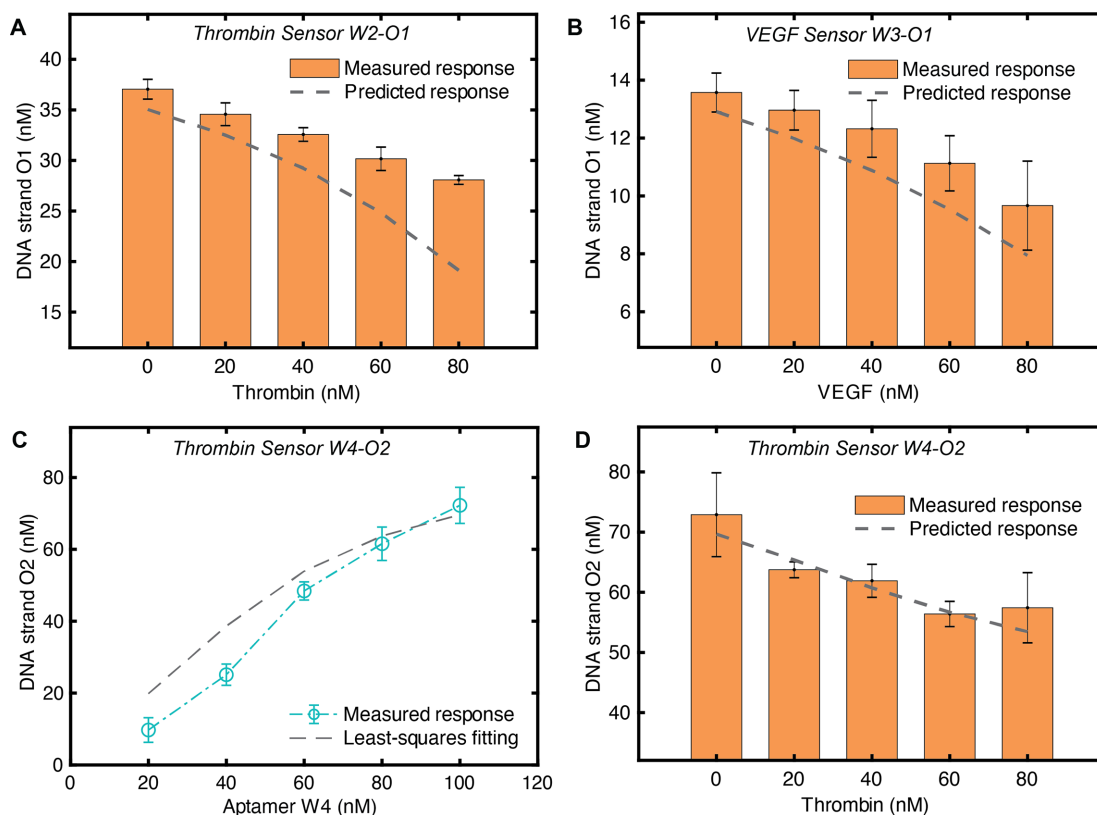
Figure 5. Different exchange processes can translate the concentrations of different input proteins into the same oligonucleotide output or the same protein into concentrations of different oligonucleotide outputs. The steady-state concentration of the output strand (*O1*) for (**A**) *Thrombin Sensor W2-O1* in response to different concentrations of thrombin where $[W2] = [X2\,Y2] = [O1Z1] = 100$ nM. (**B**) The concentration of the output strand of *VEGF Sensor W3-O1* in response to different concentrations of VEGF where $[W3] = [X3\,Y3] = [O1Z1] = 100$ nM. The *Thrombin Sensor W2-O1* used a modified TBA29 DNA aptamer that binds to thrombin (23) while *VEGF Sensor W3-O1* used a modified 3R02 DNA aptamer that binds to VEGF (38,39). Even though these exchange processes detect different proteins, they can still produce the same DNA output strand (*O1*) in response to the input proteins. For kinetic modeling of the recognition stage for each exchange process (modified TBA29-thrombin and modified 3R02-VEGF), the K_d value and forward reaction rate constant ($k_{f,1}$) of the original TBA29 (23,36) and 3R02 aptamers (38,39) were taken from the literature. The rates of the reactions involved in the transduction stage were determined in an analogous manner similar to the rates of the reactions involved in the transduction stage of the *Thrombin Sensor W1-O1* (see Supplementary Data S1). (**C** and **D**) *Thrombin Sensor W4-O2* used the same unmodified DNA aptamer (TBA15) but different *W*, *XY* and *OZ* species (*W4*, *X4Y4* and *O2Z2*) than *Thrombin Sensor W1-O1*. This distinction allowed to *Thrombin Sensor W4-O2* to modulate the concentration of the *O2* strand from *Sensor W4-O2*, which has no sequence relation to the *O1* output of *Thrombin Sensor W1-O1* (Supplementary Tables S3 and S9). (**C**) The concentration of *O2* present in response to different concentrations of the *W4* strand, where the concentrations of *X4Y4* and *O2Z2* are each 100 nM. (**D**) The response of the *Thrombin Sensor W4-O2* to different concentrations of thrombin for $[W4] = [X4] = [O2Z2] = 100$ nM. The recognition and the transduction stages of *Sensor W4-O2* were modeled in a manner to how the reactions of the *Thrombin Sensor W1-O1* were modeled (see Figure 2 and Supplementary Data S1). For both experiments, calibrations were used to convert the measured fluorescence intensities into *O1* concentrations (see Supplementary Data S3; Figures S5 and S6).

exchange processes detects only the target protein and does this using the modular transduction stages, which can accurately pass the information to a single output or different outputs.

DISCUSSION

In this paper, we constructed a sensing mechanism that produces a DNA oligonucleotide in exchange for an input protein *in situ*. The spontaneous interaction of DNA aptamers with specific proteins and their interactions with complementary DNA strands enabled the exchange processes to quickly produce outputs in the form of DNA strands that reflect the concentrations of the inputs. The sequences of the output strands can be chosen by design in a manner almost independent of choosing the sensing proteins. This independence is achieved by using a series of

toehold-mediated strand-displacement reactions that provide enough freedom to select the sequence of the output DNA oligonucleotide. Moreover, the fast, reversible nature of the cascade reactions allowed detection not only of the rise but also of the fall a protein's concentration within minutes. By appropriately choosing the initial concentrations of the sensor components, the dynamic range of the output was controlled as a function of the input. Additional control of the output dynamics of exchange processes can be achieved by placing the quencher and fluorophore molecules at the 5'-end of *Z* and 3'-end of *O* strands, respectively.

Over the past decade, a significant effort has resulted in various detection assays, which are immunosorbent (ELISA) (1,2), immunoprecipitated (40), electrochemical (41–43), mass spectrometric (3,4), plasmonic (44,45), Raman (46) and fluorescence labeling (47), that allowed to de-
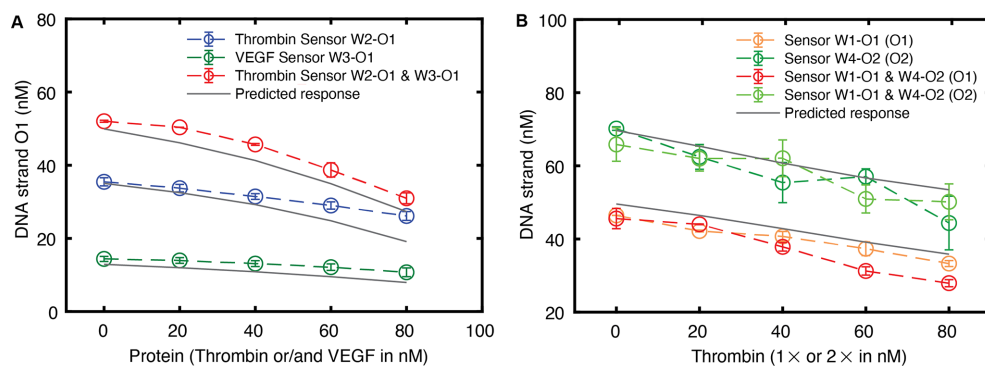
Figure 6. A single output or different outputs can be modulated concurrently in response to different proteins or the same protein, respectively. *Thrombin Sensor W2-O1 and VEGF Sensor W3-O1* detect thrombin and VEGF, respectively. Both sensors modulate the concentrations of the same output strand (*O1*) while *Thrombin Sensor W1-O1* and *Thrombin Sensor W4-O2* both detect thrombin, and modulate the concentrations of different output strands (*O1* and *O2,* respectively). (**A**) *Thrombin Sensor W2-O1* and *VEGF Sensor W3-O1* were tested concurrently for [*W2*] = [*W3*] = [*X2 Y2*] = [*X3 Y3*] = 100 nM and [*O1Z1*] = 200 nM using different amounts of thrombin and VEGF (0–80 nM) each. As a control, individual responses of each exchange process were determined in the presence of the respective sensor components ([*W2*] = [*X2 Y2*] = [*O1Z1*] = 100 nM or [*W3*] = [*X3 Y3*] = [*O1Z1*] = 100 nM) at different input protein concentrations. The combined response of the exchange processes was modeled using an ODE model that uses the same rates that were used to model the individual sensors (see Supplementary Data S1 and S7). (**B**) Likewise, the combined response of *Thrombin Sensor W1-O1* (*Z1* strand labeled with FAM fluorophore) and *Thrombin Sensor W4-O2* (*Z2* strand labeled with HEX fluorophore) was measured in the presence of [*W1*] = [*W4*] = [*X1 Y1*] = [*X4 Y4*] = [*O1Z1*] = [*O2Z2*] = 100 nM and compared with the individual responses of each exchange process at 100 nM concentration of the respective sensor components ([*W1*] = [*X1 Y1*] = [*O1Z1*] = 100 nM or [*W4*] = [*X4 Y4*] = [*O2Z2*] = 100 nM). While testing the combined operation of *Sensor W1-O1* and *Sensor W4-O2* in the same test tube, we added twice the amount of thrombin compared to the case where we tested *Sensor W1-O1* and *Sensor W4-O2* separately. A separate calibration was used to convert the measured fluorescence intensities into *O2* concentrations (see Supplementary Data S3 and Figure S7).

tect several different types of proteins and produce a readable signal in response. However, these efforts were primarily focused on improving the detection limit and did not address the challenge of performing real-time *in situ* readouts. Moreover, in these assays, the biochemical process used to detect the protein often results in the destruction of the sample. Because of these features, such assays cannot be used for real-time protein detection in a biochemical process. Our method is designed to be a solution-phase chemical circuit that can be operating *in situ* to produce an output that is a specific DNA strand sequence that could be used to drive other downstream processes.

This operation is achieved by adding additional sequences (*d* domain) in the original sequence of the aptamer that allowed to couple the recognition and transduction stages effectively. We found that adding this sequence to the aptamers we tested did not significantly increase the aptamers' K_d value. A low K_d value is desired to ensure that the concentration of free aptamer changes significantly with the changes in the protein concentration. By adding a new reaction in the transduction stage, an output strand that is completely independent of the *d* domain can be produced (Supplementary Figure S16). Improved detection sensitivity might be achieved by employing *in situ* amplification techniques (48,49). However, such changes would likely significantly decrease the speed with which the circuit could track changes in protein concentration.

One of the limitations of our approach is the need for a DNA aptamer that can reversibly bind to the protein molecule of interest with high affinity and selectivity. In recent years, there has been significant progress toward the development of new aptamers to target a wide variety of proteins (50–53); therefore, the use of DNA aptamers as affinity regent suggests a pathway to extend this scheme for detect-

ing other relevant molecules. More importantly, DNA aptamers are relatively stable at room temperature compared to RNA aptamers/antibodies, and because of this, there is a growing interest in developing DNA aptamer-based sensing assays (54,55). The use of molecular circuits can help to address some of the limitation such as off-target binding by combining the output of multiple sensors in a logical combination to identify a particular profile. This new generation of detection assays promises rapid progress toward developing stable and adaptable sensing mechanisms.

To model these exchange processes accurately, a modeling framework was developed wherein the rates of the reactions involved in the transduction stage were calculated, and further optimization through experiment or least-squares fitting was done to precisely model the protein free response. Using these rates, for each exchange process, we demonstrated that the model can accurately predict the output for a given change in the input. Note that our modeling approach requires the K_d value to model the aptamer–protein interaction, and for that we relied on the values reported in the literature for the original aptamers. However, as we have modified the original aptamers by adding a *d* domain, this modification might result in decreasing the affinity (higher K_d values) of the modified aptamers with the respective proteins. Because the predicted responses closely agreed with the measured responses for a wide range of initial conditions, it can be inferred that the K_d values for the modified aptamers should be in the same order as for the original aptamers. To test this, we varied the K_d value for each exchange process in an incremental order while keeping the other rates fixed and found a significant mismatch between the predicted response and the measured response when the K_d value was increased by a factor of five (see Supplementary Figure S17).

We have demonstrated how our approach can be easily extended to detect multiple proteins simultaneously. By exploiting the high specificity of aptamers and modular operation of the strand-displacement cascade, we were able to construct exchange processes that can produce not only the same DNA output strand in the presence of two different proteins, but also different DNA output strands in response to the same protein concurrently. An alternative scheme can be implemented to produce two different outputs in response to different input proteins (see Supplementary Figure S18). Such a multiplexed operation will be relevant in biomedical applications similar to recent work by Pierce and Dirks (48,49) where *in situ* hybridization chain reaction was used to create complex reaction cascades that provided a new platform for therapeutic interventions (56,57).

Each exchange process we designed works well separately and concurrently in a predictable manner, suggesting a robust and reliable operation of these processes and suggesting how the strategy we developed may be adopted to target other proteins or other biologically relevant molecules for which aptamers are available. Finally, the relative simplicity of this approach inspires its integration into more complex biochemical systems capable of molecular computing while detecting multiple inputs simultaneously and processing them to produce a diverse set of output responses in a manner similar to cellular signaling networks.

SUPPLEMENTARY DATA

Supplementary Data are available at NAR Online.

ACKNOWLEDGEMENTS

FUNDING

REFERENCES

1. Rissin,D.M., Kan,C.W., Campbell,T.G., Howes,S.C., Fournier,D.R., Song,L., Piech,T., Patel,P.P., Chang,L., Rivnak,A.J. *et al.* (2010) Single-molecule enzyme-linked immunosorbent assay detects serum proteins at subfemtomolar concentrations. *Nat. Biotechnol.*, **28**, 595–599.
2. Kurita,R., Arai,K., Nakamoto,K., Kato,D. and Niwa,O. (2010) Development of electrogenerated chemiluminescence-based enzyme linked immunosorbent assay for sub-pM detection. *Anal. Chem.*, **82**, 1692–1697.
3. Shi,T.J., Fillmore,T.L., Sun,X.F., Zhao,R., Schepmoes,A.A., Hossain,M., Xie,F., Wu,S., Kim,J.S., Jones,N. *et al.* (2012) Antibody-free, targeted mass-spectrometric approach for quantification of proteins at low picogram per milliliter levels in human plasma/serum. *Proc. Natl. Acad. Sci. U.S.A.*, **109**, 15395–15400.
4. Wilhelm,M., Schlegl,J., Hahne,H., Gholami,A.M., Lieberenz,M., Savitski,M.M., Ziegler,E., Butzmann,L., Gessulat,S., Marx,H. *et al.* (2014) Mass-spectrometry-based draft of the human proteome. *Nature*, **509**, 582–587.
5. Rivero-Gutiérrez,B., Anzola,A., Martínez-Augustin,O. and de Medina,F.S. (2014) Stain-free detection as loading control alternative to Ponceau and housekeeping protein immunodetection in Western blotting. *Anal. Biochem.*, **467**, 1–3.
6. Gao,W., Liu,W., Mackay,J.A., Zalutsky,M.R., Toone,E.J. and Chilkoti,A. (2009) In situ growth of a stoichiometric PEG-like conjugate at a protein's N-terminus with significantly improved pharmacokinetics. *Proc. Natl. Acad. Sci. U.S.A.*, **106**, 15231–15236.
7. Hee Choi,Y. and Yu,A.-M. (2014) ABC transporters in multidrug resistance and pharmacokinetics, and strategies for drug development. *Curr. Pharm. Des.*, **20**, 793–807.
8. Alberts,B. (1998) The cell as a collection of protein machines: preparing the next generation of molecular biologists. *Cell*, **92**, 291–294.
9. Barrios-Rodiles,M., Brown,K.R., Ozdamar,B., Bose,R., Liu,Z., Donovan,R.S., Shinjo,F., Liu,Y., Dembowy,J., Taylor,I.W. *et al.* (2005) High-throughput mapping of a dynamic signaling network in mammalian cells. *Science*, **307**, 1621–1625.
10. Yamada,T. and Bork,P. (2009) Evolution of biomolecular networks: lessons from metabolic and protein interactions. *Nat. Rev. Mol. Cell Biol.*, **10**, 791–803.
11. Wang,B.J., Barahona,M. and Buck,M. (2013) A modular cell-based biosensor using engineered genetic logic circuits to detect and integrate multiple environmental signals. *Biosens. Bioelectron.*, **40**, 368–376.
12. Weinberg,B.H., Pham,N.H., Caraballo,L.D., Lozanoski,T., Engel,A., Bhatia,S. and Wong,W.W. (2017) Large-scale design of robust genetic circuits with multiple inputs and outputs for mammalian cells. *Nat. Biotechnol.*, **35**, 453–462.
13. Antunes,M.S., Morey,K.J., Smith,J.J., Albrecht,K.D., Bowen,T.A., Zdunek,J.K., Troupe,J.F., Cuneo,M.J., Webb,C.T., Hellinga,H.W. *et al.* (2011) Programmable ligand detection system in plants through a synthetic signal transduction pathway. *PLoS One*, **6**, e16292.
14. Nandagopal,N. and Elowitz,M.B. (2011) Synthetic biology: integrated gene circuits. *Science*, **333**, 1244–1248.
15. Seelig,G., Soloveichik,D., Zhang,D.Y. and Winfree,E. (2006) Enzyme-free nucleic acid logic circuits. *Science*, **314**, 1585–1588.
16. Zhang,D.Y. and Seelig,G. (2011) Dynamic DNA nanotechnology using strand-displacement reactions. *Nat. Chem.*, **3**, 103–113.
17. Chen,Y.-J., Dalchau,N., Srinivas,N., Phillips,A., Cardelli,L., Soloveichik,D. and Seelig,G. (2013) Programmable chemical controllers made from DNA. *Nat. Nanotechnol.*, **8**, 755–762.
18. Fern,J., Scalise,D., Cangialosi,A., Howie,D., Potters,L. and Schulman,R. (2017) DNA strand-displacement timer circuits. *ACS Synth. Biol.*, **6**, 190–193.
19. Li,F., Zhang,H.Q., Lai,C., Li,X.F. and Le,X.C. (2012) A Molecular Translator that Acts by Binding-Induced DNA Strand Displacement for a Homogeneous Protein Assay. *Angew Chem. Int. Edit.*, **51**, 9317–9320.
20. Engelen,W., Meijer,L.H.H., Somers,B., de Greef,T.F.A. and Merkx,M. (2017) Antibody-controlled actuation of DNA-based molecular circuits. *Nat. Commun.*, **8**, 14473.
21. Li,B.L., Ellington,A.D. and Chen,X. (2011) Rational, modular adaptation of enzyme-free DNA circuits to multiple detection methods. *Nucleic Acids Res.*, **39**, e110.
22. Kong,J.L., Zhu,J.B., Chen,K.K. and Keyser,U.F. (2019) Specific Biosensing Using DNA Aptamers and Nanopores. *Adv. Funct. Mater.*, **29**, 1807555.
23. Han,D., Zhu,Z., Wu,C., Peng,L., Zhou,L., Gulbakan,B., Zhu,G., Williams,K.R. and Tan,W. (2012) A logical molecular circuit for programmable and autonomous regulation of protein activity using DNA aptamer–protein interactions. *J. Am. Chem. Soc.*, **134**, 20797–20804.
24. Gan,H.Y., Wu,J. and Ju,H.X. (2019) Proximity hybridization-induced on particle DNA walker for ultrasensitive protein detection. *Anal. Chim. Acta*, **1074**, 142–149.
25. De Silva,A.P. and Uchiyama,S. (2007) Molecular logic and computing. *Nat. Nanotechnol.*, **2**, 399–410.
26. Agrawal,D.K., Franco,E. and Schulman,R. (2015) A self-regulating biomolecular comparator for processing oscillatory signals. *J. Royal Soc. Interf.*, **12**, 20150586.
27. Agrawal,D.K., Marshall,R., Noireaux,V. and Sontag,E.D.(2019) In vitro implementation of robust gene regulation in a synthetic biomolecular integral controller. *Nat. Commun.*, **10**, 5760.

28. Zhang,D.Y. and Winfree,E. (2009) Control of DNA strand displacement kinetics using toehold exchange. *J. Am. Chem. Soc.*, **131**, 17303–17314.

29. Nutiu,R. and Li,Y. (2003) Structure-switching signaling aptamers. *J. Am. Chem. Soc.*, **125**, 4771–4778.

30. Zadeh,J.N., Steenberg,C.D., Bois,J.S., Wolfe,B.R., Pierce,M.B., Khan,A.R., Dirks,R.M. and Pierce,N.A. (2011) NUPACK: analysis and design of nucleic acid systems. *J. Comput. Chem.*, **32**, 170–173.

31. Baldrich,E., Restrepo,A. and O'Sullivan,C.K. (2004) Aptasensor development: elucidation of critical parameters for optimal aptamer performance. *Anal. Chem.*, **76**, 7053–7063.

32. Bajzar,L., Morser,J. and Nesheim,M. (1996) TAFI, or plasma procarboxypeptidase B, couples the coagulation and fibrinolytic cascades through the thrombin-thrombomodulin complex. *J. Biol. Chem.*, **271**, 16603–16608.

33. Bock,L.C., Griffin,L.C., Latham,J.A., Vermaas,E.H. and Toole,J.J. (1992) Selection of single-stranded DNA molecules that bind and inhibit human thrombin. *Nature*, **355**, 564.

34. Li,J.J., Fang,X. and Tan,W. (2002) Molecular aptamer beacons for real-time protein recognition. *Biochem. Biophys. Res. Commun.*, **292**, 31–40.

35. Goji,S. and Matsui,J. (2011) Direct detection of thrombin binding to 8-bromodeoxyguanosine-modified aptamer: Effects of modification on affinity and kinetics. *J. Nucleic Acids*, **2011**, 316079.

36. Tasset,D.M., Kubik,M.F. and Steiner,W. (1997) Oligonucleotide inhibitors of human thrombin that bind distinct epitopes. *J. Mol. Biol.*, **272**, 688–698.

37. Paborsky,L., McCurdy,S.N., Griffin,L.C., Toole,J.J. and Leung,L. (1993) The single-stranded DNA aptamer-binding site of human thrombin. *J. Biol. Chem.*, **268**, 20808–20811.

38. Hasegawa,H., Sode,K. and Ikebukuro,K. (2008) Selection of DNA aptamers against VEGF165 using a protein competitor and the aptamer blotting method. *Biotechnol. Lett.*, **30**, 829–834.

39. Nonaka,Y., Yoshida,W., Abe,K., Ferri,S., Schulze,H., Bachmann,T.T. and Ikebukuro,K. (2012) Affinity improvement of a VEGF aptamer by in silico maturation for a sensitive VEGF-detection system. *Anal. Chem.*, **85**, 1132–1137.

40. Jain,A., Liu,R.J., Ramani,B., Arauz,E., Ishitsuka,Y., Ragunathan,K., Park,J., Chen,J., Xiang,Y.K. and Ha,T. (2011) Probing cellular protein complexes using single-molecule pull-down. *Nature*, **473**, 484–488.

41. Landry,M.P., Ando,H., Chen,A.Y., Cao,J.C., Kottadiel,V.I., Chio,L., Yang,D., Dong,J.Y., Lu,T.K. and Strano,M.S. (2017) Single-molecule detection of protein efflux from microorganisms using fluorescent single-walled carbon nanotube sensor arrays. *Nat. Nanotechnol.*, **12**, 368–377.

42. Taleat,Z., Cristea,C., Marrazza,G., Mazloum-Ardakani,M. and Sandulescu,R. (2014) Electrochemical immunoassay based on aptamer-protein interaction and functionalized polymer for cancer biomarker detection. *J. Electroanal. Chem.*, **717**, 119–124.

43. Hammock,M.L., Knopfmacher,O., Naab,B.D., Tok,J.B.H. and Bao,Z.A. (2013) Investigation of protein detection parameters using nanofunctionalized organic field-effect transistors. *ACS Nano*, **7**, 3970–3980.

44. Zijlstra,P., Paulo,P.M.R. and Orrit,M. (2012) Optical detection of single non-absorbing molecules using the surface plasmon resonance of a gold nanorod. *Nat. Nanotechnol.*, **7**, 379–382.

45. Ament,I., Prasad,J., Henkel,A., Schmachtel,S. and Sonnichsen,C. (2012) Single Unlabeled Protein Detection on Individual Plasmonic Nanoparticles. *Nano Lett.*, **12**, 1092–1095.

46. Yang,X., Gu,C., Qian,F., Li,Y. and Zhang,J.Z. (2011) Highly sensitive detection of proteins and bacteria in aqueous solution using surface-enhanced raman scattering and optical fibers. *Anal. Chem.*, **83**, 5888–5894

47. Sakabe,M., Asanuma,D., Kamiya,M., Iwatate,R.J., Hanaoka,K., Terai,T., Nagano,T. and Urano,Y. (2013) Rational design of highly sensitive fluorescence probes for protease and glycosidase based on precisely controlled spirocyclization. *J. Am. Chem. Soc.*, **135**, 409–414.

48. Dirks,R.M. and Pierce,N.A. (2004) Triggered amplification by hybridization chain reaction. *Proc. Natl. Acad. Sci. U.S.A.*, **101**, 15275–15278.

49. Choi,H.M.T., Chang,J.Y., Trinh,L.A., Padilla,J.E., Fraser,S.E. and Pierce,N.A. (2010) Programmable in situ amplification for multiplexed imaging of mRNA expression. *Nat. Biotechnol.*, **28**, 1208–1212.

50. Stoltenburg,R., Reinemann,C. and Strehlitz,B. (2007) SELEX—a evolutionary method to generate high-affinity nucleic acid ligands. *Biomol. Eng.*, **24**, 381–403.

51. Zhuo,Z.J., Yu,Y.Y., Wang,M.L., Li,J., Zhang,Z.K., Liu,J., Wu,X.H., Lu,A.P., Zhang,G. and Zhang,B.T. (2017) Recent Advances in SELEX Technology and Aptamer Applications in Biomedicine. *Int. J. Mol. Sci.*, **18**, 2142.

52. Ng,E.W.M., Shima,D.T., Calias,P., Cunningham,E.T., Guyer,D.R. and Adamis,A.P. (2006) Pegaptanib, a targeted anti-VEGF aptamer for ocular vascular disease. *Nat. Rev. Drug Discov.*, **5**, 123–132.

53. Cowperthwaite,M.C. and Ellington,A.D. (2008) Bioinformatic analysis of the contribution of primer sequences to aptamer structures. *J. Mol. Evol.*, **67**, 95–102.

54. Zhou,W.Z., Huang,P.J.J., Ding,J.S. and Liu,J. (2014) Aptamer-based biosensors for biomedical diagnostics. *Analyst*, **139**, 2627–2640.

55. Dunn,M.R., Jimenez,R.M. and Chaput,J.C. (2017) Analysis of aptamer discovery and technology. *Nat. Rev. Chem.*, **1**, 0076.

56. Jung,C. and Ellington,A.D. (2014) Diagnostic Applications Applications of Nucleic Acid Circuits. *Acc. Chem. Res.*, **47**, 1825–1835.

57. Wu,C.C., Wan,S., Hou,W.J., Zhang,L.Q., Xu,J.H., Cui,C., Wang,Y.Y., Hu,J. and Tan,W.H. (2015) A survey of advancements in nucleic acid-based logic gates and computing for applications in biotechnology and biomedicine. *Chem. Commun.*, **51**, 3723–3734.